[Article ID] 1003- 6326(2001)05- 0784- 06

Study on bioleaching of refractory gold ore (Ⅰ)①

——Mechanism on bioleaching of pyrite by *Thiobacillus ferrooxidans*

MIN Xiao-bo(闵小波)[1], CHAI Li-yuan(柴立元)[1], CHEN Wei-liang(陈为亮)[1], ZHANG Chuan-fu(张传福)[1], HUANG Bai-yun(黄伯云)[2], KUANG Zhong(邝 中)[3]

(1. Department of Metallurgical Science & Engineering, Central South University, Changsha 410083, P. R. China;
2. State Key Laboratory for Powder Metallurgy, Central South University, Changsha 410083, P. R. China;
3. Guangxi Guanghe Industry Co. Lt., Hechi 547000, P. R. China)

[Abstract] The variation of main parameters including ion concentration, pH value, potential and biomass was examined in bioleaching pyrite. The pH value of the solution decreased obviously. Most of *T. ferrooxidans* adhered to the surface of pyrite. The surface properties of pyrite and leached products were determined by SEM, EDS and XRD. Pyrite was corroded selectively by *T. ferrooxidans* and sulfur in pyrite was leached preferentially. The primary product for bioleaching pyrite was jarosite. Based on these results, it can be found that pyrite is oxidized mainly through the direct role of *T. ferrooxidans*. A band model for bioleaching pyrite was built, by which the bioleaching process was explained theoretically. The model shows that the holes, which are injected into the valence band of pyrite through adhered *T. ferrooxidans*, result from dissolved oxygen in the solution.

[Key words] mechanism; pyrite bioleaching; *Thiobacillus ferrooxidans*

[CLC number] TF18 **[Document code]** A

1 INTRODUCTION

Studies on the growth[1~3] and applications[4] of *Thiobacillus ferrooxidans* have been carried out by many researchers, since it is one of the most important micro-organisms for the recovery of some metals including copper and uranium from low-grade ores in industrial heap, dump, and in situ leaching processes in the early period. And recently, it has been applied for pretreatment of refractory sulfide gold ores[4~6]. In this case, bacteria are essentially used for the oxidation of gold-bearing pyrite (FeS_2) and arsenopyrite (FeAsS). The biooxidation of these sulfide minerals allows the release of the dispersed microinclusions of native gold.

Generally, the biological effect can be divided into two categories, direct and indirect metabolic reactions, leading to two mechanisms of contact. The direct mechanism requires physical contact between bacteria and pyrite particles, and the biooxidation of pyrite will give rise to sulfate acid and ferric iron, which are expressed by Eq. (1). In the indirect contact mechanism, the bacteria oxidize ferrous ion to the ferric state, thereby regenerating the ferric ion required for chemical oxidation of pyrite (Eq. (2))[7].

$$4FeS_2 + 15O_2 + 2H_2O \xrightarrow{\text{Bacteria}} 2Fe_2(SO_4)_3 + 2H_2SO_4 \quad (1)$$

$$FeS_2 + 7Fe_2(SO_4)_3 + 8H_2O \xrightarrow{\text{Chemical}} 15FeSO_4 + 2H_2SO_4 \quad (2)$$

Despite extensive studies on the bacterial leaching of refractory sulfide gold concentrates containing pyrite in recent years[8~10], the mechanisms of pyrite bacterial oxidation are not well understood[11,12]. This study is aimed at clarifying the mechanism of pyrite biooxidation through investigation of the behavior of pyrite bioleaching, including physicochemical composition of leachate, the evolution of corrosion patterns, and the nature of surface-oxidized chemical species.

2 MATERIALS AND METHODS

2.1 Experimental device

Bioleaching experiments were performed in stirred pulp reactors, which consisted of 1.5 L glass flasks and Teflon turbines used to stir (500 r/min) and oxygenate the medium efficiently (0.2 ~ 0.3 L/min air). The reactors were immersed in a thermoregulated water bath maintained at 303 K. The flask contained initially 1 L of culture medium and 20 g pure pyrite to obtain a pulp density of 2%.

Samples of growth suspensions were treated with hydrochloric acid to have final acid concentrations of approximately 3 mol/L and then were left for 30 min at room temperature. The metal concentrations in

① [Received date] 2001- 04- 02; [Accepted date] 2001- 05- 27

these extracts are described as "total" metal concentrations, and the metal concentrations in untreated extracts are described as "soluble" metal concentrations. The ferrous iron and ferric iron concentration were determined by model 720 spectrophotometer. The solution potential was measured by platinum electrode versus a saturated calomel electrode.

2.2 Bacteria and nutrient medium

The bacterium *Thiobacillus ferrooxidans* was provided by the Chinese Academy of Science. The medium for the bacterial culture and the reactor experiment consisted of 0.45 g/L $(NH_4)_2SO_4$, 0.15 g/L K_2HPO_4, 0.5 g/L $MgSO_4 \cdot 7H_2O$, 0.05 g/L KCl, 0.01 g/L $Ca(NO_3)_2$, and was adjusted to pH 2.0 with sulfuric acid. The reactor setup was inoculated with an actively growing culture to have an initial population of 10^7 bacteria per milliliter. Free bacteria in the leaching solution were measured by direct microscopic counting using a haemacytometer.

2.3 Mineral sample

The pyrite used for this experiment was prepared from large pure natural crystals originating from Chinese Geology Museum. Iron and sulfur contents were, respectively, of 45.28% and 50.07% (mass fraction). After being washed with 6 mol/L HCl solution, the pyrite crystals were carefully dry-ground in a tungsten mill and wet-sieved in order to obtain a particle fraction of 53~ 80 μm.

2.4 Microscopy observations

The massive samples of pyrite were prepared by inclusion of small piece of mineral (between 0.8 and 1.0 cm diameter) for the observations by SEM and EDS using KYKY-2800 microscopes with Finder-100. During experiment, the massive pyrite sample was introduced into the flask, attached to the stopper by a tantalum bridle to maintain its position in the leaching process.

In addition, powder samples were dried at O_2-free atmosphere to preserve the surface for XRD analysis using an X-ray Diffraction D-5000.

3 BEHAVIOR OF PYRITE BIOLEACHING

3.1 Evolution of iron concentration

The results of iron concentration in solution versus time during pyrite bioleaching are shown in Fig. 1. Initially, since the bacterial growth was in the lag phase, iron solubilization was very weak, and no detectable evolution was noted. Though ferric iron existed in solution, there was no pyrite oxidation by it. At the second step, the bioleaching process began, and the solubilization of iron became significant. The third step was dominated by the differences between the soluble iron concentration and the total iron concentration, which shows that iron precipitation produced in reactor. Because of this, the oxidation of pyrite was inhibited.

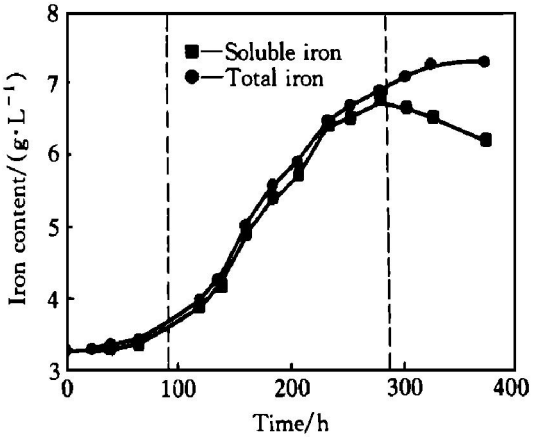

Fig. 1 Evolution of iron contents during pyrite bioleaching

Fig. 2 is a plot of the ferrous iron contents in solution versus time during pyrite bioleaching. For a start, a little ferrous iron solubilization resulted from the chemical solubilization of pyrite in nutrient medium (about 0.25g/L). With the beginning of the exponential growth phase, the ferrous ions produced were quickly oxidized, and the ferrous iron concentration tended to decrease. From 140 h to 300 h, it approximated to zero. After 300 h, the ferrous iron concentration increased slightly.

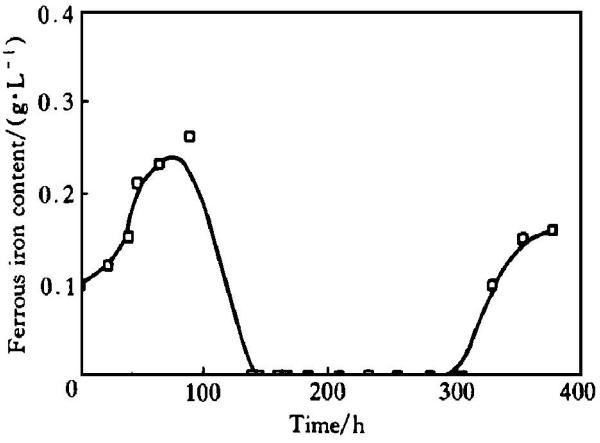

Fig. 2 Ferrous iron contents in solution vs time during pyrite bioleaching

3.2 Evolution of pH value

The evolution of pH during pyrite bioleaching is given in Fig. 3. Since 100 h, the pH decreased gradually from initial value 2.2 to final value 1.35. The main reason is considered that the bacterial oxidation of pyrite is an acid-yielding process, except for the form of the precipitation.

3.3 Evolution of solution potential during pyrite bioleaching

The evolution of solution potential is presented in

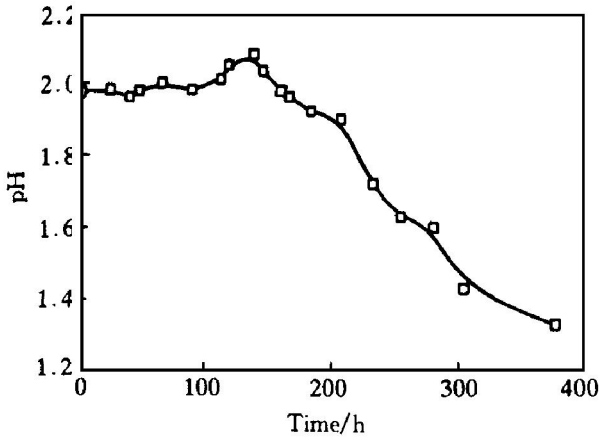

Fig. 3 Evolution of pH during pyrite bioleaching

Fig. 4. From 0 h to 100 h, the solution potential stabilized at 510~ 520 mV, after 100 h, it increased and reached a stable value of 600 mV.

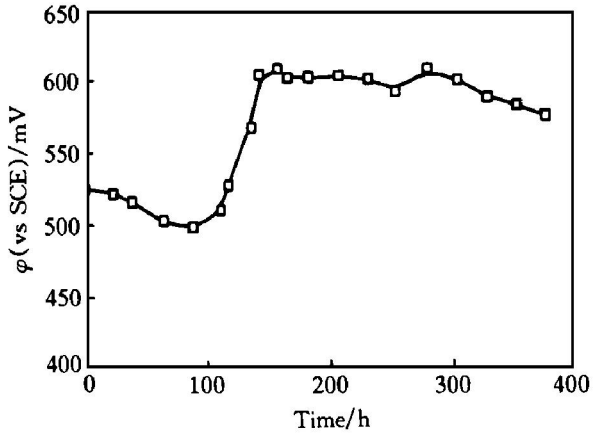

Fig. 4 Evolution of solution potential during pyrite bioleaching

3.4 Evolution of bacterial population

Fig. 5 shows the bacterial population growth in the pyrite bioleaching. The number of bacteria in the liquid medium decreased. Adsorption onto pyrite, which involved 90% of inoculated bacteria, began immediately after the inoculation. The number of bacteria in the nutrient medium increased with the exponential growth phase and reached a stable value of 10^9 bacteria/mL.

3.5 SEM, EDS and XRD analysis of pyrite

SEM photographs showing the evolution of the surface of pyrite during the bioleaching process are seen in Fig. 6. A clean surface and no corrosion pattern were detectable initially by SEM examination at high magnification (×2500) (Fig. 6(a)). At 120 h, the first patterns of corrosion were evident from the appearance of some cracks, which seemed to be related to the fragility zones of layer and to its crystallographic orientations (in Fig. 6(b)). At 250 h, deep and oriented corrosion pores, which pass through the

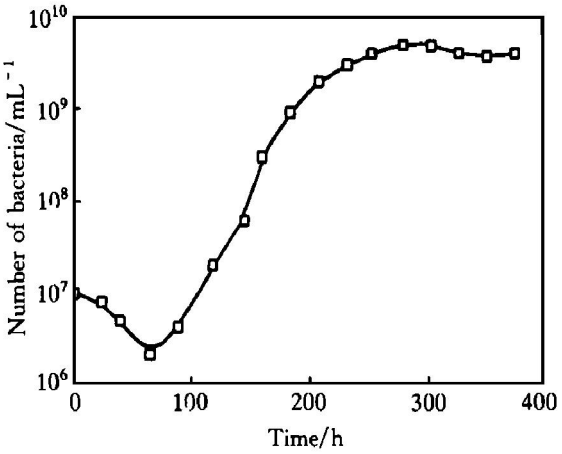

Fig. 5 Bacterial population growth during pyrite bioleaching

pyrite layer, were evident and the corrosion feature can be called selective corrosion. At the end of bioleaching, the surface of the pyrite was completely covered by a coarse pellicular phase (Fig. 6(d)).

The results of energy dispersive spectra analysis of pyrite surface in bioleaching are given in Fig. 7 and Table 1. According to the variation of stoichiometric composition of sulfur in pyrite, it can be determined that the preferential oxidation composition in pyrite is sulfur. Fig. 8 shows the X-ray diffractogram of pyrite powder after bioleaching. Bacterial leaching led to the concurrent precipitation of one minerals, jarosite [$KFe_3(SO_4)_2(OH)_6$], and no element sulfur could be detected.

4 MECHANISM OF PYRITE BIOLEACHING

The characteristics of pyrite bioleaching are listed in Table 2. On the base of these bioleaching characteristics, the mechanism of pyrite bioleaching can be ascertained. As noted above, the mechanism of bioleaching can be divided into two kinds: direct and indirect mechanism. Which mechanism is the most important in pyrite bioleaching? The pyrite is oxidized by ferric iron to ferrous iron. Simultaneously, it is unavoidable that the ferric iron will be reduced to ferrous iron, so a great deal of ferrous ions will produce. Assuming the indirect oxidation is the most important, it is contradictive to the experimental results that no ferrous iron can be detectable during bioleaching. To say the least, even if bacteria can catalyze the ferrous iron oxidation to ferric iron so quickly that no ferrous iron is in solution. However, the oxidation of ferrous iron to ferric iron is an acidconsuming reaction, which will result in increase of solution pH value. But the experimental results show the contrary phenomenon. The results of EDS analysis show that the preferential oxidation substance was sulfur in pyrite which was oxidized to sulfate by *T. ferrooxidans* directly, and no element sulfur was detectable

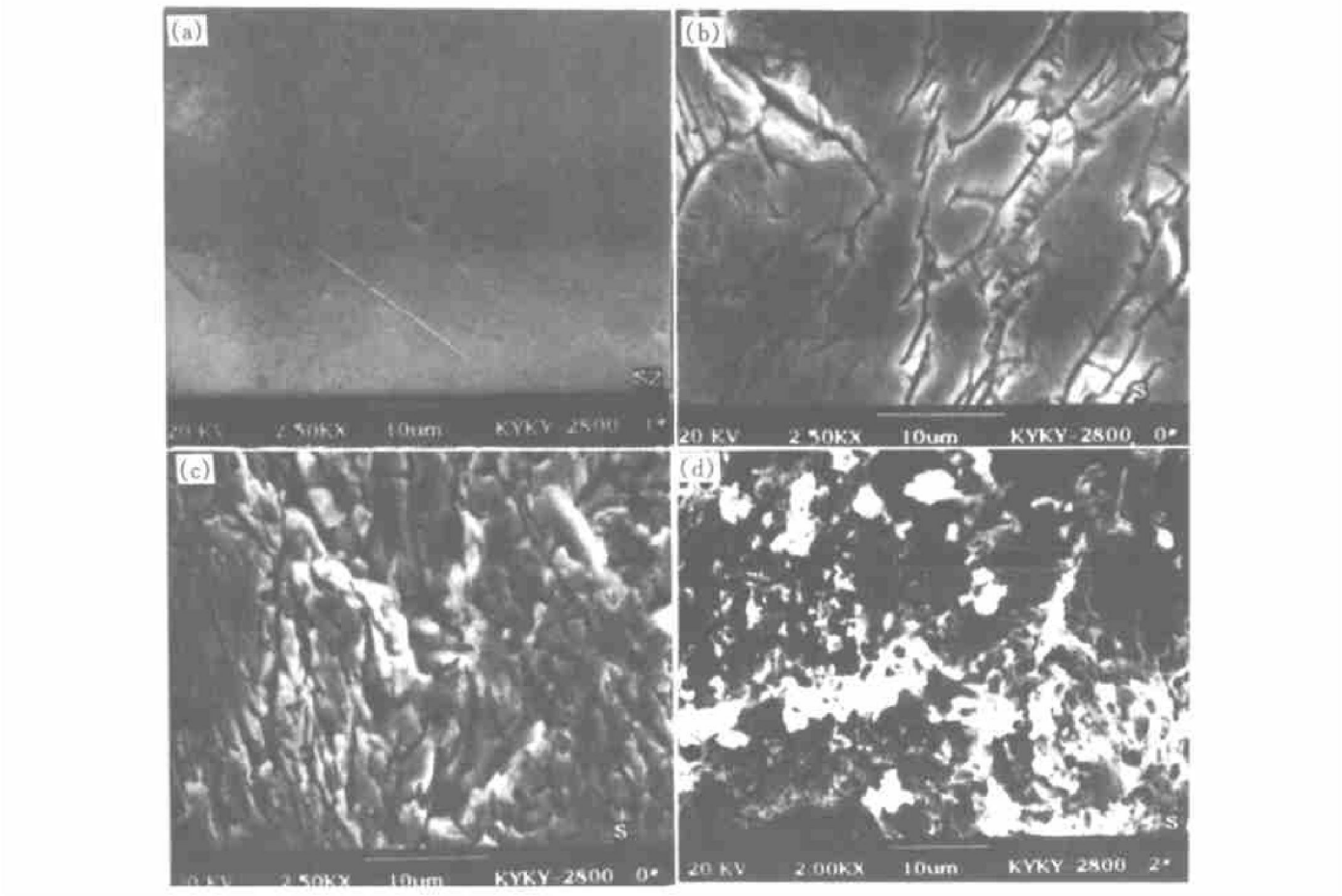

Fig. 6 SEM photographs of surface of pyrite in bioleaching process
(a) —Initial pyrite surface; (b) —Massive pyrite surface attacked for 120 h;
(c) —Massive pyrite surface attacked for 250 h; (d) —Massive pyrite surface attacked for 380 h

Table 1 EDS analysis results of pyrite surface during bioleaching

No.	Composition	Content (mass fraction) / %	Content (mole fraction) / %	Stoichiometric composition
a	Fe S	48.09 54.91	34.72 65.28	$FeS_{1.88}$
b	Fe S	57.84 41.62	44.02 55.17	$FeS_{1.25}$
c	Fe S	49.34 50.66	35.86 64.14	$FeS_{1.78}$

Table 2 Characteristics of pyrite bioleahcing

Iron leaching rate	0.029 g/(L•h)
Evolution of pH	Decreasing markedly, from 2.0 to 1.35
Evolution of potential	Increasing to a stable value of 600 mV
Bacteria growth	Bacteria adhering on pyrite surface, final biomass 10^9 bacteria/mL
Corrosion feature	Selective corrosion
Preferential oxidation	Sulfur in pyrite
Element sulfur	No element sulfur produced
Precipitation	Jarosite

by XRD. In addition, it is the base of direct oxidation that bacteria are adhering on the surface of pyrite, which is proved by the SEM observation that the corrosion pattern of bioleaching pyrite is selective. Through the discussion above, it can be concluded that the direct oxidation mechanism is the most important in bioleaching pyrite.

5 BAND MODEL OF PYRITE

In solid state physics, energy levels are usually expressed in unit of electron volt (eV), the reference state is taken as the energy of the free electron at infinity (vacuum), which is arbitrarily set at zero value. The eV scale of energy levels may be related to the conventional electrochemical potential E_h (V) scale as[13]:

$$E/\mathrm{eV} = -eE_h/\mathrm{V} - 4.5 \quad (3)$$

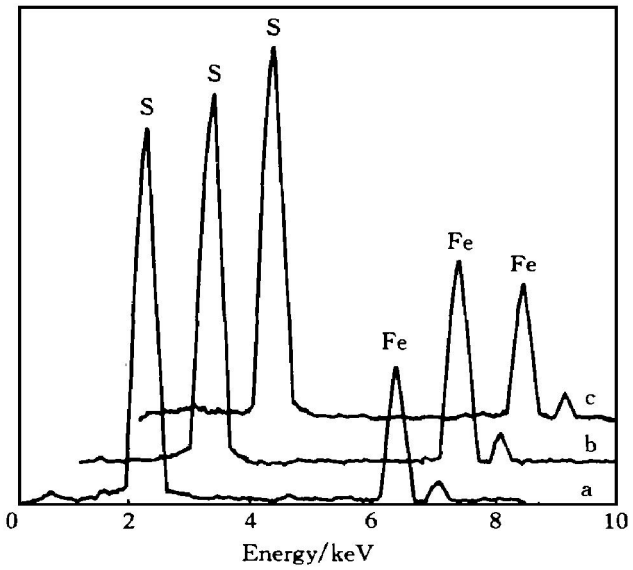

Fig. 7 EDS analysis of pyrite surface during bioleahcing
a —Initial pyrite surface;
b —Massive pyrite surface attacked for 120 h;
c —Massive pyrite surface attacked for 250 h

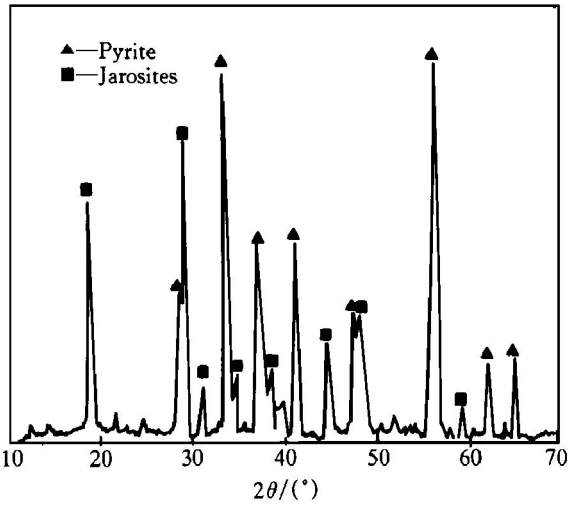

Fig. 8 X-ray diffractogram of pyrite powder after bioleaching

where e represents the electronic charge. Thus, relative to vacuum scale, the standard hydrogen electrode represents an energy level at − 4.5 eV. Using Eq. (3) it is possible to express redox and electrode potential in terms of energy levels, as illustrated in Fig. 9. For example, Fe^{3+}/Fe^{2+} couple standard electrode potential is 0.77 V, so in the band model, its energy levels is − 0.77 eV.

The energy of the bottom of conduction band (E_c) is defined by Eq. (4)[14]:

$$E_c = 4.5 - \chi \quad (4)$$

where χ is the electron affinity. It was calculated according to Eq. (5):

$$\chi = X - 1/2E_g \quad (5)$$

where X and E_g are semiconductor electronegativity and band gap respectively. X can be calculated by the following Eqs. (6) and (7)[15].

$$W = 1.794X_p + 1.11 \quad (6)$$

$$X(FeS_2) = [W(Fe) + 2W(S)]/3 \quad (7)$$

$$E_c - E_v = E_g \quad (8)$$

where W and X_p are work function and Pauling electronegativity, E_v is the energy of the top of valence band.

Table 3 lists the basic parameters for pyrite band model. According to this parameters and equation, the band model can be built (see Fig. 9).

Direct mechanism is the most important in pyrite bioleaching. In pyrite/solution band model (Fig. 9), the energy level of Fe^{3+}/Fe^{2+} couple is in the band gap of pyrite, it is unfavorable for electron transfer or

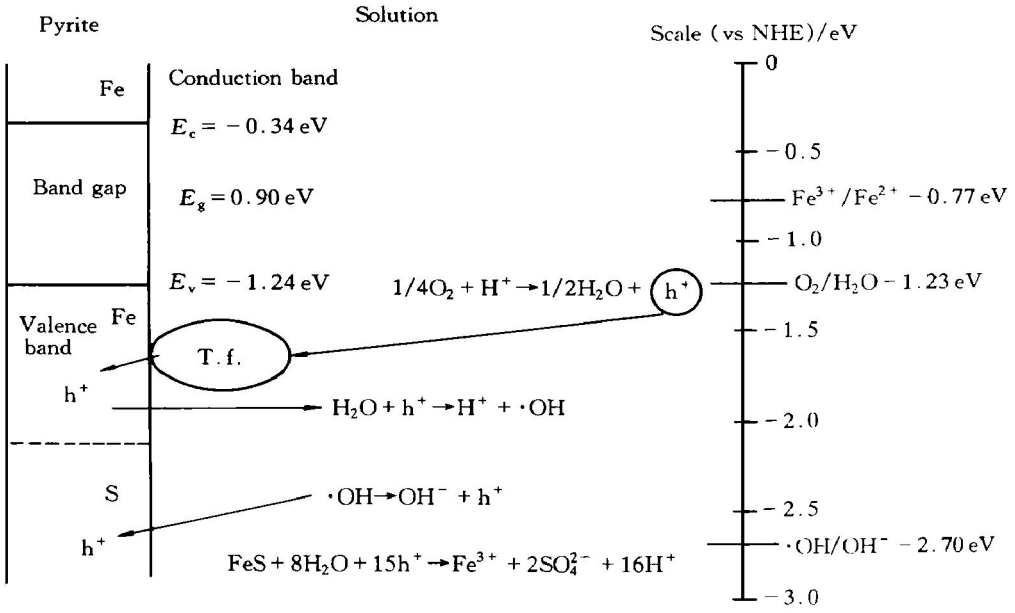

Fig. 9 Band model of pyrite bioleaching (direct oxidation mechanism)

Table 3 Basic parameters for pyrite band model (eV)

Element	X_p	W			
S	2.58	5.74			
Fe	1.83	4.39			
Mineral	X	χ	E_g [15, 16]	E_c	E_v
FeS_2	5.29	4.84	0.9	− 0.34	− 1.24
FeAsS	5.05	4.85	0.4	− 0.35	− 0.75

hole exchange, so that it is impossible for ferric iron to oxidize the pyrite. The process of bioleaching pyrite can be described as follows: *T. ferrooxidans* is adhering on the surface of pyrite, and transfer the electron from pyrite to oxygen. It leads to the results that the holes which inject into the valence band of pyrite through adhered *T. ferrooxidans*, result from dissolved oxygen in the solution. But pyrite is that the valence band is narrow and of non-bonding character, electron transfer with this band (hole injection) will therefore have no effect on the structure or bonding of the pyrite, and corrosion will not come about[16]. Holes in the valence band of pyrite are capable of oxidizing water, and subsequently of producing •OH, which is an intermediate hydroxide radical. The •OH radical is a strong oxidizing agent and reacts directly with the sulfur valence band to form sulfate.

6 CONCLUSIONS

As for bioleaching process of pyrite, the pH value of the solution decreased obviously. Most of *T. ferrooxidans* adhered to the surface of pyrite. The attack of bacteria makes the preferential oxidation of sulfur in pyrite to sulfate, and no element sulfur is produced. After attack by bacteria, the corrosion pattern shows the feature of selective corrosion. Based on these results, it can be found that pyrite is oxidized mainly through the direct role of *T. ferrooxidans*, i. e. the direct oxidation mechanism is the most important in bioleaching pyrite.

[REFERENCES]

[1] Chai L, Wei W, Okido M. Studies on effect of Cu(II) on growth of *Thiobacillus ferrooxidans* using series piezoelectric quartz crystal [J]. Minerals Engineering, 2000, 13(8-9): 969-972.

[2] MIN Xiao-bo, CHAI Li-yuan, ZHONG Hai-yun, et al. Kinetic parameters for growth of *T. Ferrooxidans* [J]. The Chinese Journal of Nonferrous Metals, (in Chinese), 2000, 10(3): 443-447.

[3] ZHANG Chuan-fu, MIN Xiao-bo, CHAI Li-yuan, et al. Influencing factors of lag phase in growth of *T. Ferrooxidans* [J]. Journal of Central South University of Technology, (in Chinese), 1999, 30(5): 492-496.

[4] Brieriey L. Bacterial oxidation [J]. Engineering and Mining Journal, 1995, 196(5): 42-44.

[5] Van Aswegen P C. Developments and innovations in bacterial oxidation of refractory ores [J]. Minerals and Metallurgical Processing, 1991, 8(4): 188-191.

[6] Brown A R G, Irvine W, Odd P A R. Bioleaching-Wiluna operating experience [J]. Biomine, 1994, 9

[7] Holmes D S. Biorecovery of metals from mining, industrial and urban wastes [A]. Martin A M. Bioleaching of sulfide for recovery of gold, Ind. Min., 1998, 19(3-4): 26-29.

[8] Komnitsas C, Pooley F D. Optimization of the bacterial oxidation of an arsenical gold sulphide concentrate from Olympias, Greece [J]. Minerals Engineering, 1991, 4(12): 1297-1303.

[9] Groudev S N, Spasova I I, Ivanov I M. Two-stage microbial leaching of a refractory gold-bearing pyrite ore [J]. Minerals Engineering, 1996, 9(7): 707-713.

[10] Barrett J, Hughes M N. Mechanism of the bacterial oxidation of arsenopyrite-pyrite mixtures: the identification of plant control [J]. Minerals Engineering, 1993, 6(8-10): 969-975.

[11] Holmes P R, Fowler T A, Crundwell F K. The mechanism of bacterial action in the leaching of pyrite by *Thiobacillus ferrooxidans*: An electrochemical study [J]. J Electrochem Soc, 1999, 146(8): 2906-2912.

[12] Osseo-Asare K. Semiconductor electrochemistry and hydrometallurgical dissolution process [J]. Hydrometallurgy, 1992, 29: 61-90.

[13] Frese K W Jr. Simple method for estimating energy levels of solids [J]. J Vac Sci Technol, 1979, 16(4): 1042-1044.

[14] Butler M A, Ginley D S. Prediction of flatband potential at semiconductor-electrolyte interface from atomic electronegativities [J]. J Electrochem Soc, 1978, 125(2): 228-232.

[15] Tributsch H, Bennett J C. Semiconductor-electrochemical aspect of bacterial leaching (I). Oxidation of metal sulfides with large energy gap [J]. J Chem Tech Biotechnol, 1981, (31): 565-577.

[16] Crundwell F K. The influence of the electronic structure of solids on the anodic dissolution and leaching of semiconducting sulphide minerals [J]. Hydrometallurgy, 1988, 21: 155-190.

(Edited by YUAN Sai-qian)